

## A Note on High/Low-Wave-Number Interactions in Spatially Discrete Parabolic Equations

ANDREW STUART†

Department of Mathematics, Massachusetts Institute of Technology,  
Massachusetts 02139, USA

[Received 30 June 1988]

We describe an instability introduced by the spatial discretization of reaction-diffusion equations. The mechanism is a nonlinear interaction between high and low wave-number modes in the discrete equations. In partial differential equations which exhibit strong temporal growth, a parasitic high-wave-number mode is stimulated, through aliasing, by a physically meaningful low-wave-number mode. We analyse the interaction using phase-plane techniques and present complementary numerical results.

### 1. Introduction

IN THIS note we analyse nonlinear instabilities caused by spatial discretizations of reaction-diffusion equations of the form

$$u_t = u_{xx} + f(u), \quad (\text{P})$$

for  $x \in (0, 1)$ , together with either periodic or Neumann boundary conditions. In particular we shall focus on the case in which

$$f(u) = a + bu + cu^2 + eu^3,$$

for real  $a, b, c, e$ . We discuss the form of initial conditions later.

We introduce a spatial mesh by the points  $x_j = j\Delta x$  for  $j = 0, \dots, J$ , where  $J\Delta x = 1$ . We denote our approximation to  $u(x_j, t)$  by  $U_j(t)$ . Using the standard three-point approximation to  $u_{xx}$ , we obtain the system of ordinary differential equations

$$\frac{dU_j}{dt} = \frac{\delta_x^2 U_j}{\Delta x^2} + f(U_j) \quad (\text{PD})$$

for  $j = 0, \dots, J$ , together with appropriate discretizations of the boundary conditions which determine  $U_{-1}(t)$  and  $U_{J+1}(t)$ . Here  $\delta_x^2 U_j = U_{j+1} - 2U_j + U_{j-1}$ .

The problem of nonlinear instability in numerical approximations of partial differential equations is the subject of a great deal of current research. Much of the explicit analysis focuses on non-dissipative discretizations of hyperbolic problems (particularly the inviscid Burgers' equation) and is motivated by the important papers [7, 16]. More recent references include [2, 3, 18, 20]. Such problems can exhibit violent instabilities caused by the nonlinear self-interaction

† Present address: School of Mathematical Sciences, University of Bath, Bath BA2 7AY, UK.

of a high-wave-number mode. Since neither the underlying partial differential equation nor its discretization possess an inherent damping mechanism, these instabilities are particularly severe. Milder instabilities caused by a weak resonance between high- and low-wave-number modes have been identified by Moore [14] in equations modelling water waves; recent work [3] suggests a relationship between Moore's mechanism and the behaviour of leap-frog discretizations of Burgers' equation.

The study of nonlinear instability in the discretization of dissipative partial differential equations has received less attention since the damping mechanism in the underlying equation tends to counteract instabilities (see [6] for an analysis of the viscous Burgers' equation which is relevant for small viscosities or large-amplitude initial data). However, there is a well-known linear instability mechanism in discrete parabolic equations [17] which arises when the Courant number  $\Delta t/\Delta x^2$  exceeds  $\frac{1}{2}$ ; ten years ago Newell [15] showed how nonlinear effects could be incorporated into this mechanism, by employing a discrete multiple-scales analysis along the lines of the weakly nonlinear theories of hydrodynamic stability [5, 12]. The linear instability mechanism is associated with the growth of a high-wave-number mode, and the nonlinear effects can either exacerbate the instability or balance it to produce spurious time-oscillatory behaviour or more complicated bounded dynamics [13, 15, 19]. Recent work by the author [19], based on the ideas of Newell [15], describes a related instability arising in discretizations of reaction-diffusion equations in which the reaction term can act as a source of energy to a low-wave-number mode. The instability is caused by an interaction between the physically meaningful low-wave-number mode and a spurious (poorly resolved) high-wave-number mode.

However, whilst the work in [19] applies to a very broad class of nonlinearities  $f(u)$ , it is limited in a fundamental way: the analysis is based on local bifurcation theory and requires that two parameters be close to their critical values. None the less, the work suggests that high/low-wave-number interactions are important in discrete parabolic equations and it is the purpose of this paper to demonstrate that the interactions arise in a global fashion, without parameter restrictions, in a wide class of equations which exhibit finite-time singularities. The instability considered here is entirely nonlinear in character and is not a modification of linear theories. Furthermore, whilst the instability described in [19] is caused by *time discretization*, this note is concerned purely with instabilities introduced by *spatial discretization*. Typical examples of nonlinearly unstable computations are shown in Figs 3 to 5 where a spurious mode with spatial period  $3\Delta x$  is generated.

In section 2 we show that the semidiscrete problem (PD) admits closed-form solutions comprising only three spatial modes. For appropriate initial conditions this enables us to reduce (PD) to a low-dimensional system of coupled ordinary differential equations. In section 3 we discuss the behaviour of this system by phase-plane analysis. Section 4 contains a brief analysis of (P) for comparison with (PD). We present numerical experiments with (PD), which indicate the relevance of our analysis, in section 5. In section 6 we make some concluding remarks.

**2. 3-mode solutions of (PD)**

In this section we show that (PD) admits closed solutions of the form

$$U_j(t) = A(t) \exp(2\pi ij/3) + A^*(t) \exp(-2\pi ij/3) + B(t), \tag{2.1}$$

where \* denotes complex conjugation. This solution comprises a  $3\Delta x$ -periodic mode superimposed on a spatially uniform one. For the moment we ignore the boundary conditions on the problem. The solution (2.1) is admitted as a result of the property of *aliasing*, namely that on a discrete grid large classes of periodic functions are indistinguishable from one another. In particular, we use the following relations, where equality holds for integer  $j$  (that is, equality denotes ‘indistinguishable when sampled on the discrete grid’):

$$\exp(-4\pi ij/3) = \exp(2\pi ij/3); \quad \exp(4\pi ij/3) = \exp(-2\pi ij/3); \quad \exp(\pm 2\pi ij) = 1. \tag{2.2}$$

Using equations (2.1), (2.2) we can establish the following relationships:

$$U_j^3 = B^3 + A^3 + A^{*3} + 3[A^2A^* + A^{*2}B + AB^2] \exp(2\pi ij/3) + 3[AA^{*2} + A^2B + A^*B^2] \exp(-2\pi ij/3) \tag{2.3}$$

and

$$U_j^2 = B^2 + 2AA^* + [A^{*2} + 2AB] \exp(2\pi ij/3) + [A^2 + 2A^*B] \exp(-2\pi ij/3). \tag{2.4}$$

Straightforward trigonometric identities demonstrate that

$$\delta_x^2[\exp(2\pi ij/3)] = -3 \exp(2\pi ij/3) \quad \text{and} \quad \delta_x^2[\exp(-2\pi ij/3)] = -3 \exp(-2\pi ij/3). \tag{2.5}$$

Substituting (2.1) and (2.3) to (2.5) into (PD) and equating the coefficients of the three distinct modes (which can be justified by discrete orthogonality conditions), we obtain a third-order dynamical system (assuming that  $B(t)$  is real) defined by

$$\frac{dA}{dt} = \left( \frac{b\Delta x^2 - 3}{\Delta x^2} \right) A + c[A^{*2} + 2AB] + 3e[A^2A^* + A^{*2}B + AB^2], \tag{2.6}$$

$$\frac{dB}{dt} = a + bB + c[B^2 + 2AA^*] + e[B^3 + A^3 + A^{*3}]. \tag{2.7}$$

In the original partial differential equation one would expect the nonlinearity to produce a cascade of energy to smaller and smaller scales. However, the aliasing prevents this and permits the closed form of solution (2.1). The feedback mechanism caused by aliasing was first identified by Phillips in a discretization of the barotropic vorticity equation [16].

We now discuss boundary conditions. We assume that  $J$  is a multiple of 3. Then (2.1) satisfies (PD) together with the discrete *periodicity* conditions

$$U_{-1}(t) = U_{J-1}(t) \quad \text{and} \quad U_{J+1}(t) = U_1(t). \tag{2.8}$$

If we specify the discrete *homogeneous Neumann* boundary conditions

$$U_1(t) = U_{-1}(t) \quad \text{and} \quad U_{J+1}(t) = U_{J-1}(t), \quad (2.9)$$

then (2.1) satisfies (PD) and (2.9) provided that  $A(t)$  is real. In this case the third-order dynamical system reduces to a pair of ordinary differential equations. We shall concentrate on this case in the following section.

If (P) is solved subject to periodic or homogeneous Neumann boundary conditions, together with spatially uniform initial data, then the solution  $u(x, t)$  remains constant in space for all time and satisfies the ordinary differential equation

$$\frac{du}{dt} = a + bu + cu^2 + eu^3. \quad (2.10)$$

Equations (2.6), (2.7) represent the solution of (PD) subject to the same initial condition; thus the equation (2.7) for  $B(t)$  is the spatially discrete version of (2.10). The evolution of the pair  $(A(t), B(t))$ , representing the high- and low-wave-number modes respectively, is crucial to determining the validity of approximating (P) by (PD). Of particular interest is how small initial values of  $A(t)$  (representing rounding or truncation errors) evolve in time.

### 3. Phase-plane analysis

In this section we analyse equations (2.6), (2.7) with  $A(t)$  real, in the phase plane; these equations represent the solution of (PD) subject to the discrete Neumann conditions (2.9). The inhibiting effect of dissipation on the instability mechanism can be clearly seen from the  $O(\Delta x^{-2})$  damping term on the right-hand side of equation (2.6). The question of interest is whether strong growth in the physical mode  $B(t)$  can stimulate growth in the spurious mode  $A(t)$  by nonlinear interaction, thus overcoming the effect of dissipation. Consequently we shall concentrate on parameter values for  $a, b, c, e$  which ensure rapid growth of the physical mode. Such growth is determined by the highest-order nonlinearity and so we shall concentrate on the cases when  $a = b = c = 0, e > 0$ ; and  $a = b = e = 0, c > 0$ . These cases isolate the two dominant nonlinear effects. In section 5 we present numerical results for more general sets of parameter values which justify the claim that cases (i) and (ii) define the dominant behaviour in (PD).

*Case (i):*  $a = b = c = 0; e > 0$

From equation (2.10) we deduce that  $u(x, t)$ , the solution of (P), satisfies

$$u(x, t) = \frac{u_0}{(1 - 2eu_0^2 t)^{\frac{1}{2}}}, \quad (3.1)$$

where  $u_0$  denotes the spatially uniform initial value. Thus  $u(x, t)$  remains spatially uniform and becomes unbounded at finite time  $t_c = 1/2eu_0^2$ . We compare this behaviour with that of (PD) defined by (2.1), (2.6), (2.7) with  $A(t)$  real.

In this case equations (2.6), (2.7) reduce to

$$\frac{dA}{dt} = 3A[e(A^2 + AB + B^2) - 1/\Delta x^2], \tag{3.2}$$

$$\frac{dB}{dt} = e[B^3 + 2A^3]. \tag{3.3}$$

The critical points of this system are given by  $(0, 0)$  and  $(\pm p, \mp 2^{1/3}p)$ , where

$$p = [\Delta x^2 e(1 - 2^{1/3} + 2^{2/3})]^{-1/2}.$$

The origin represents the trivial stationary solution of (P) whilst the outer critical points are spurious equilibria generated by the spatial discretization. The origin is nonlinearly unstable and the two outer equilibria are spiral repellers.

Figure 1 shows the phase diagram for equations (3.2), (3.3). (The diagram can be extended to negative  $A(t)$  by noting that (3.2), (3.3) are invariant under  $A \rightarrow -A$  and  $B \rightarrow -B$ .) Notice the trajectories along the  $B$ -axis, which represent the true solution subject to spatially uniform initial conditions. All other trajectories, however, lead eventually to growth in the spurious mode  $A(t)$  so that it becomes of the same order as  $B(t)$ . Analysis of (3.2), (3.3) shows that, for large  $A(t)$ ,  $B(t) \approx qA(t)$ , where  $q$  satisfies  $2q^3 + 3q^2 + 3q = 2$ . This cubic has a single real solution, namely  $q = 0.429445$ .

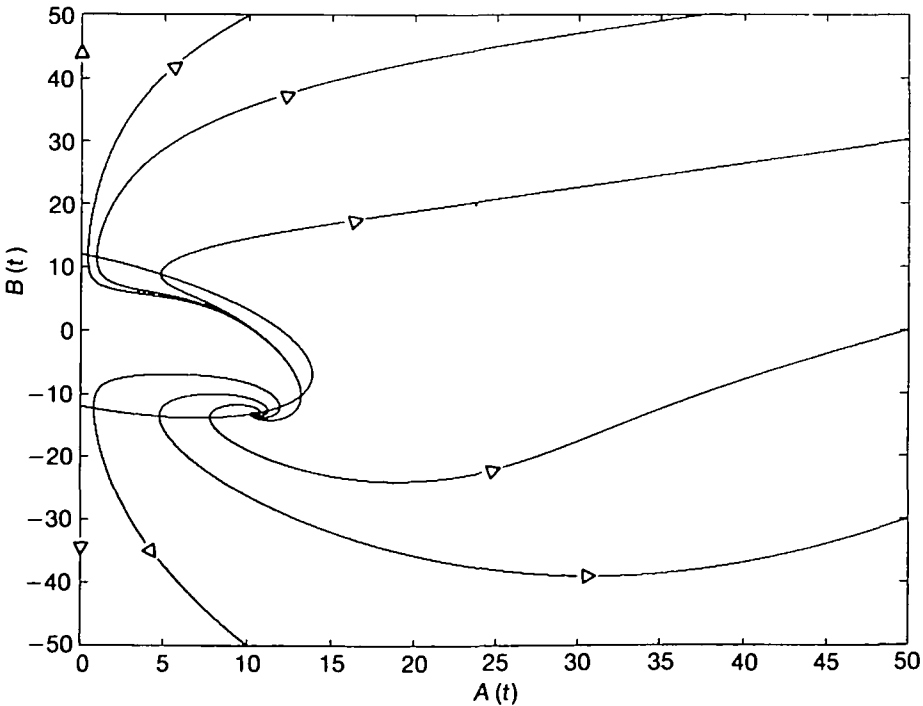


FIG. 1. Phase diagram for equations (3.2), (3.3) and the critical ellipse (3.4).  $\Delta x = \frac{1}{12}$  and  $e = 1$

Typically we can expect rounding and truncation errors to introduce small perturbations to the spatially uniform system. These perturbations will contain a component of the spurious  $3\Delta x$ -periodic spatial mode. We can analyse the effect of such small errors by considering trajectories which start close to the  $B$ -axis. For simplicity let us consider initial data in the first quadrant. It is clear from equation (3.2) that  $A(t)$  is a decreasing function of time until the ellipse

$$e(A^2 + AB + B^2) = \Delta x^{-2} \quad (3.4)$$

is traversed—see Fig. 1. This occurs for  $B(t) = O(\Delta x^{-1})$ . Since  $B(t)$  approximates  $u(t)$  accurately until this time (since  $A(t)$  is small), we are justified in deducing that the growth of  $A(t)$  becomes significant for  $t - t_c = O(\Delta x^2)$ , assuming that  $B(0) = O(1)$ . This follows from (3.1) with  $u(x, t) = O(\Delta x^{-1})$ .

This is a small time region. However, the spatial structure of finite time singularities in partial differential equations is a subject of much current interest [4, 8, 10, 11] and this analysis serves as a warning that, close to the blow-up time, even time-exact numerical methods are prone to spurious behaviour caused purely by the spatial discretization. An indication of the extreme care required to compute successfully close to the blow-up time can be found in [1].

*Case (ii):  $a = b = e = 0; c > 0$*

From equation (2.10) we deduce that  $u(x, t)$ , the solution of (P), satisfies

$$u(x, t) = \frac{u_0}{(1 - ctu_0)}. \quad (3.5)$$

Thus  $u(x, t)$  becomes unbounded in finite time  $t_c = 1/cu_0$ , if  $u_0 > 0$ .

Equations (2.6), (2.7), governing the evolution of  $A(t)$  and  $B(t)$ , reduce to

$$\frac{dA}{dt} = A[cA + 2cB - 3/\Delta x^2], \quad (3.6)$$

$$\frac{dB}{dt} = c[B^2 + 2A^2]. \quad (3.7)$$

The origin is the only equilibrium point and is nonlinearly unstable; thus the phase diagram is uninteresting. Again the solution along the  $B$ -axis represents the true spatially uniform solution. As in case (i),  $A(t)$  eventually grows to become of the same magnitude as  $B(t)$ , and equations (3.6), (3.7) indicate that  $B(t) \approx A(t)$  or  $-2A(t)$ , for  $A(t) \gg 1$ .

Confining our attention to the first quadrant we see from (3.6) that, after small initializations, the growth of  $A(t)$  becomes significant for  $B(t) = O(\Delta x^{-2})$ , when  $dA/dt$  changes sign. Since  $B(t)$  approximates  $u(t)$  adequately until this time, we deduce from equation (3.5) that the growth of  $A(t)$  is again significant for  $t - t_c = O(\Delta x^2)$ , at which point  $B(t) \approx u(x, t) = O(\Delta x^{-2})$ . Thus the results of both cases (i) and (ii) lead to the same conclusion about the time-scales on which the nonlinear instability is significant.

**4. Linear stability analysis for (P)**

In this section we analyse the stability of spatially uniform solutions of (P) under small perturbations. We show that the spatially uniform solutions are unstable but that the character of the instability differs entirely from that in (PD) described in section 3—it is initially a linear phenomenon, dominated by low-wave-number activity.

For simplicity we consider case (i) for which the spatially uniform solution is given by equation (3.1). We also take homogeneous Neumann boundary conditions. If we linearize (P) about this solution, then the small perturbation  $v(x, t)$  satisfies the equation

$$v_t = v_{xx} + \frac{3eu_0^2}{(1 - 2etu_0^2)} v, \tag{4.1}$$

subject to the boundary conditions

$$v_x(0, t) = v_x(1, t) = 0. \tag{4.2}$$

These equations (4.1), (4.2) can be solved by separation of variables to give

$$v(x, t) = \frac{\sum_{k=1}^{\infty} r_k \exp(-k^2\pi^2 t) \cos(k\pi x)}{(1 - 2etu_0^2)^{\frac{1}{2}}}. \tag{4.3}$$

Clearly all the modes in this solution eventually grow in time, since each one becomes unbounded as  $t$  approaches  $t_c$ . Since the growth of  $v(x, t)$  is more rapid than the growth of the spatially uniform solution (3.1) it is reasonable to deem the spatially uniform solution unstable. However, the instability is not appreciable until  $t$  is close to  $t_c$ . In fact, a given mode  $\cos(k\pi x)$  becomes comparable to the spatially uniform solution (3.1) for  $t = t_c - \tau_k$ , where  $\tau_k = O(\exp(-k^2\pi^2 t_c))$ . Thus, whilst all modes grow eventually in time, the low-wave-number modes dominate the process and nonlinear effects come into effect before the high wave numbers are excited by purely linear effects. Thus we expect the initial evolution of instabilities in the partial differential equation to be governed by growth of low-wave-number modes.

**5. Numerical results**

Here we present some numerical results which confirm the validity of the analysis in sections 3 and 4. The computations were done on equations (PD) subject to the boundary conditions (2.9). We emphasize that the instabilities we have described are purely a product of the *spatial* discretization and so we choose a numerical time-integration routine with the purpose of minimizing the temporal discretization error. In this way we avoid the problem of instability caused by temporal discretization, which is not the subject of this note. (A preliminary study of the effect of temporal discretization *could* be initiated by studying the recurrence relations resulting from discretization of the ordinary differential equations (2.6), (2.7).)

The equations (PD) were solved by the forward Euler method with the time step  $\Delta t$  chosen at each time level to satisfy

$$\Delta t = \Delta x^2 / (Cu_{\max}^{r-1}). \quad (5.1)$$

Here  $u_{\max}$  is the maximum over  $j$  of the approximations to the functions  $U_j(t)$  at that time level, and  $r$  is the degree of the polynomial  $f(u)$ . This choice of time step is made for two reasons.

(i) The scaling  $\Delta t \propto \Delta x^2$  in (5.1) follows from linearized numerical stability theory for Euler's method in the neighbourhood of some representative constant solution of  $O(1)$  with respect to the mesh-spacings. In this case, which is relevant to the initial evolution of the problem from  $O(1)$  data, the stability requirements are determined purely by the parabolic heat operator and lower-order terms in the differential equation can be ignored [17].

(ii) As the solution becomes large, the linearized criterion given above, which relies on the balance between spatial and temporal derivatives in (P), ceases to be relevant; the important balance becomes that between the time derivative and the nonlinear source term. Considering these terms alone, scaling shows that  $O(1)$  relative changes in the magnitude of the solution occur on a time scale of  $O(u_{\max}^{1-r})$ , when  $u_{\max}$  is large. Thus we choose the time step in (5.1) to reflect this time scale. Such a scaling is employed by Hocking *et al.* [9] in a case with  $r = 3$ , but with different boundary conditions.

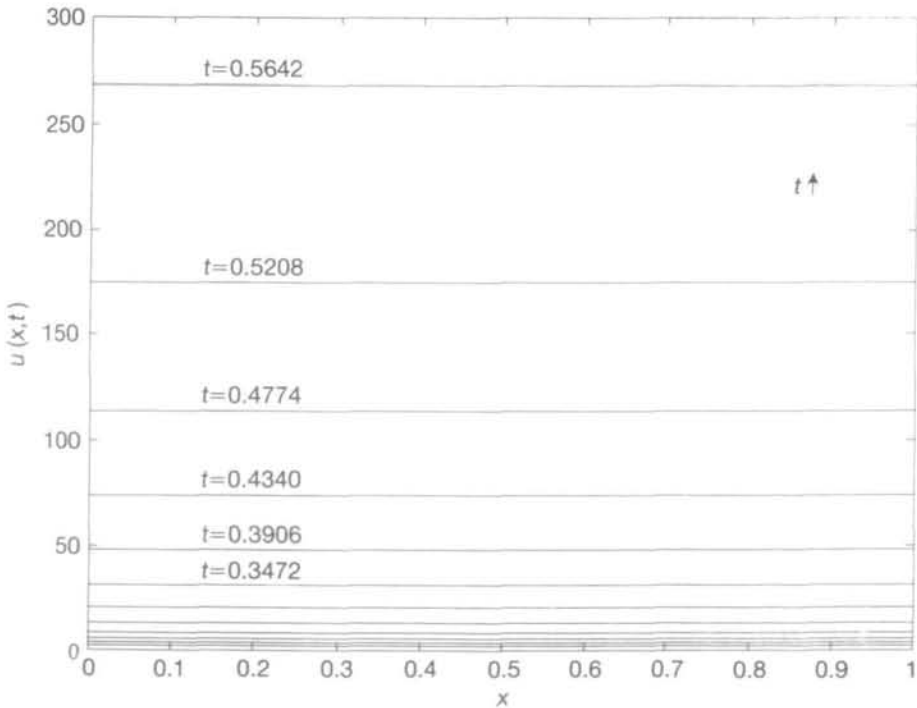


FIG. 2. Solutions of (PD), with  $J = 12$  and  $f(u) = 10u$ . Profiles at intervals of  $25\Delta t$

We claim that for these two reasons our choice of time step (5.1) for Euler's method is the maximum possible choice consistent with the aim of eliminating *temporal* discretization errors. The final validation of this claim comes from the agreement between the theory and numerical experiments.

With an explicit method a spatially uniform initial distribution remains uniform at all time steps. Thus to simulate the effect of rounding and truncation error, which would destroy the spatial uniformity of solutions if an implicit time-stepping algorithm was used, we use initial data which is a small perturbation of a constant value. In Fig. 2 the constant  $C$  in (5.1) is 4 and in Figs 3 to 8 it is 6.94. In Fig. 2 the times at which the solutions are graphed are printed next to each profile. In Figs 3 to 8 the time given is the blow-up time for the numerical method; since the interesting behaviour is compressed into a time region within  $O(\Delta x^2)$  of the blow-up time, it is not necessary to label each profile individually.

In Figs 2, 3 and 4 we use the initial conditions  $U_j(0) = 1 + 10^{-5} \cos(2\pi j/3)$ . The profiles are graphed at intervals of 25 time steps. Figure 2 shows the case when  $f(u) = 10u$ . There is no nonlinear interaction in this case and the solution develops in a spatially uniform fashion, after the initial non-uniformities are damped out. Notice that the solution evolves exponentially in time, in agreement with the spatially uniform solution  $u(x, t) = e^{10t}$ —the relative error in the last profile is about five per cent.

Figure 3 shows results in the case  $f(u) = 5u^3$  and  $\Delta x = \frac{1}{12}$ . The data for Fig. 4

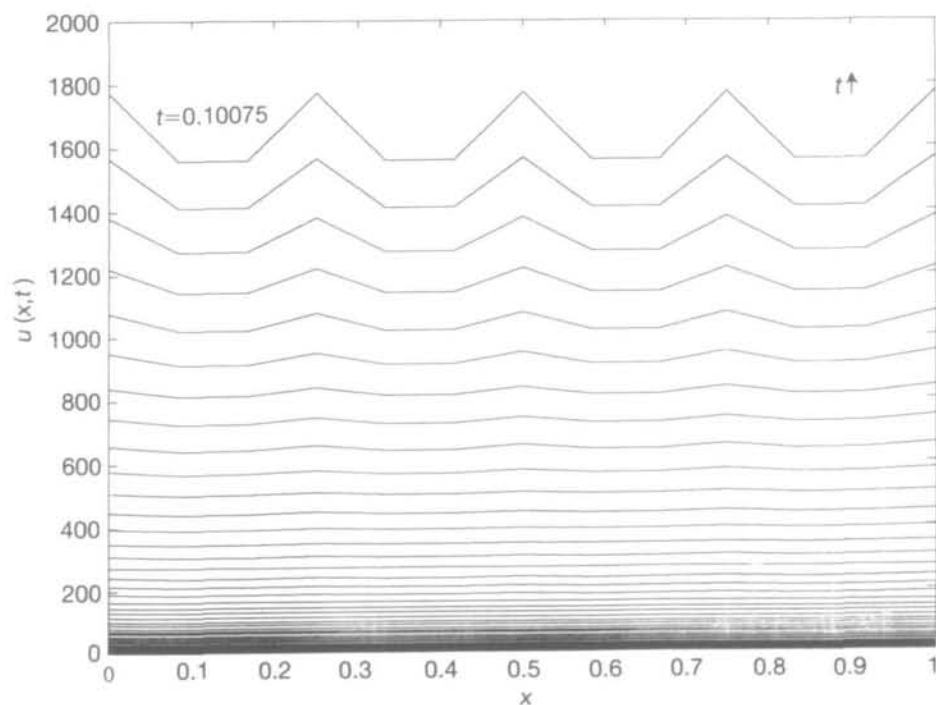


FIG. 3. Solutions of (PD), with  $J = 12$  and  $f(u) = 5u^3$ . Profiles at intervals of  $25\Delta t$

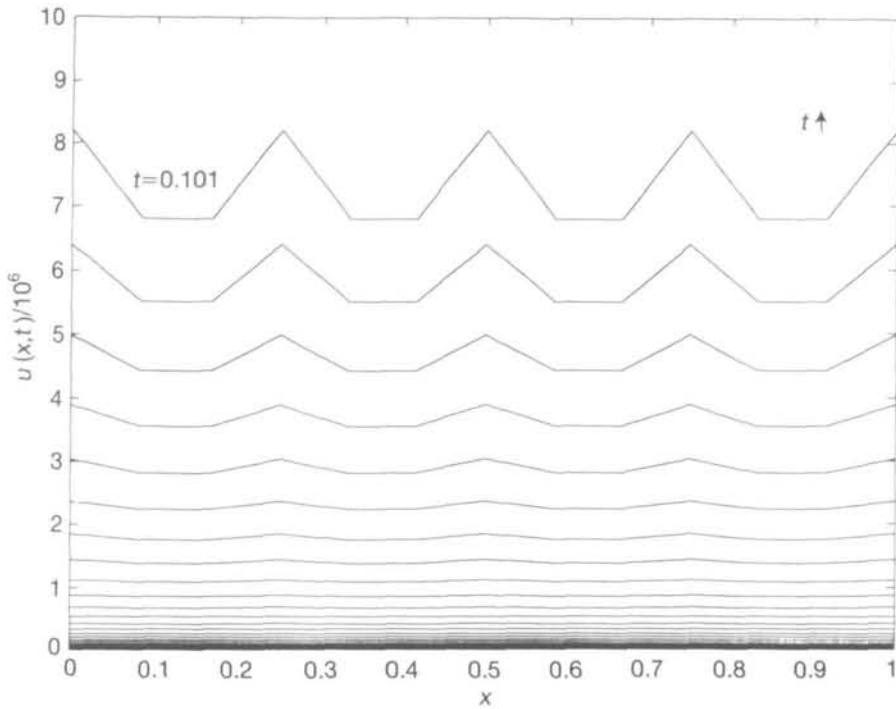


FIG. 4. Solutions of (PD), with  $J = 12$  and  $f(u) = 10u^2$ . Profiles at intervals of  $25\Delta t$

are the same as for Fig. 3, except for the nonlinearity which is of the form  $f(u) = 10u^2$ . The growth of the parasitic wave with period  $3\Delta x$  is clear, and is in accordance with the analysis in section 3. The data for Fig. 5 are identical to those used in Fig. 3 except that the nonlinearity is now  $f(u) = 5(u^3 - u^2)$  and  $U_j(0) = 2 + 10^{-5} \cos(2\pi j/3)$ . In this case the phase plane for the 3-mode solution is a modification of that shown in Fig. 1 to allow for two additional (unstable) fixed points  $(A(t), B(t)) = (0, \pm 1)$ . The numerical results indicate that the qualitative results about the behaviour near to the blow-up time  $t = t_c$  are preserved under modifications of the lower-order terms in the cubic  $f(u)$ .

For Fig. 6 we changed the initial data to  $U_j(0) = 1.0 + 10^{-5} \cos(\pi j/J)$ . This corresponds to a small spatially non-uniform perturbation proportional to the most unstable mode in the partial differential equation (P), according to the linear theory in section 4. Otherwise the data are identical to those used for Fig. 3. The results show a focusing near to  $x = 0$ , caused by the slight perturbation to the initial conditions; this behaviour reflects a genuine property of the partial differential equation.

In Fig. 7 we used the same conditions as for Fig. 3 except that

$$U_j(0) = 1 + 10^{-5} \cos(\pi j/2).$$

The solution evolves into a spatial structure with period  $4\Delta x$ ; this suggests the existence of closed solutions similar to (2.1) but with a longer period. In Fig. 8 we

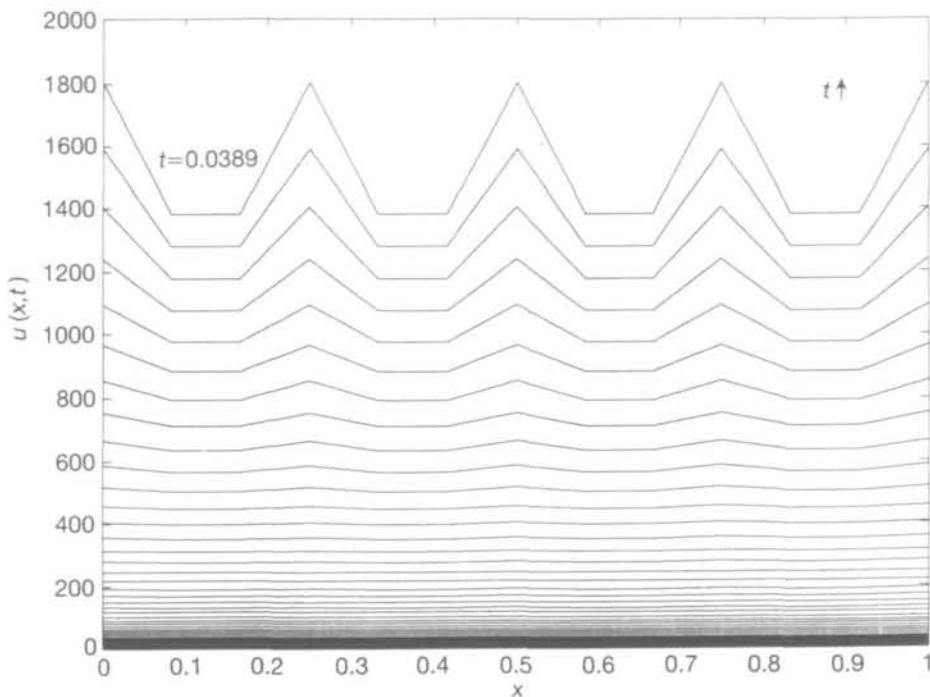


FIG. 5. Solutions of (PD), with  $J = 12$  and  $f(u) = 5(u^3 - u^2)$ . Profiles at intervals of  $25\Delta t$

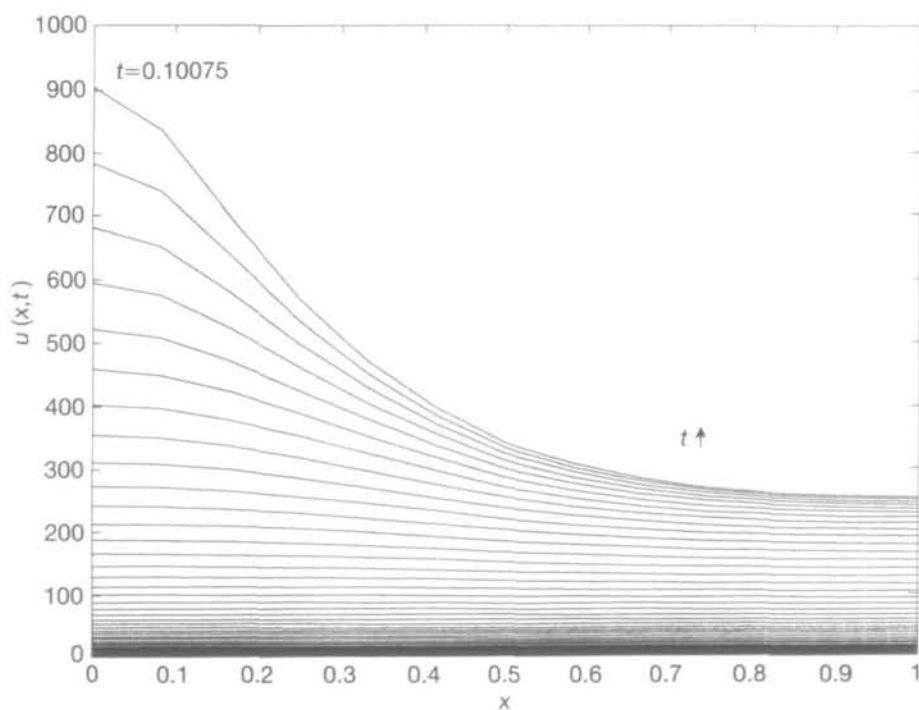


FIG. 6. Solutions of (P) with  $f(u) = 5u^3$ . Profiles at intervals of  $25\Delta t$

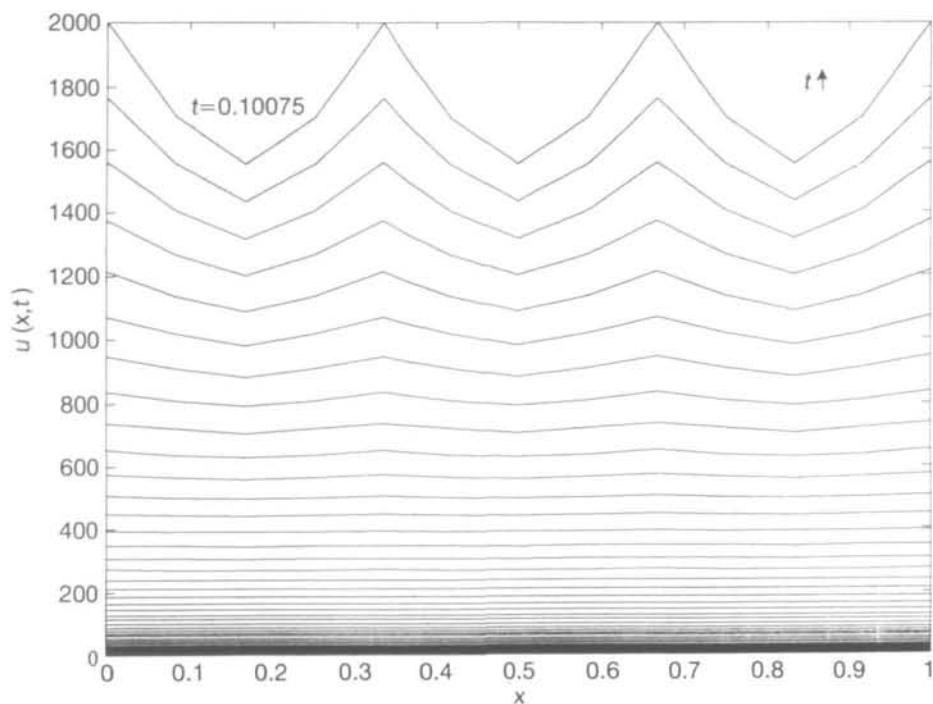


FIG. 7. Solutions of (PD), with  $J = 12$  and  $f(u) = 5u^3$ . Profiles at intervals of  $25\Delta t$

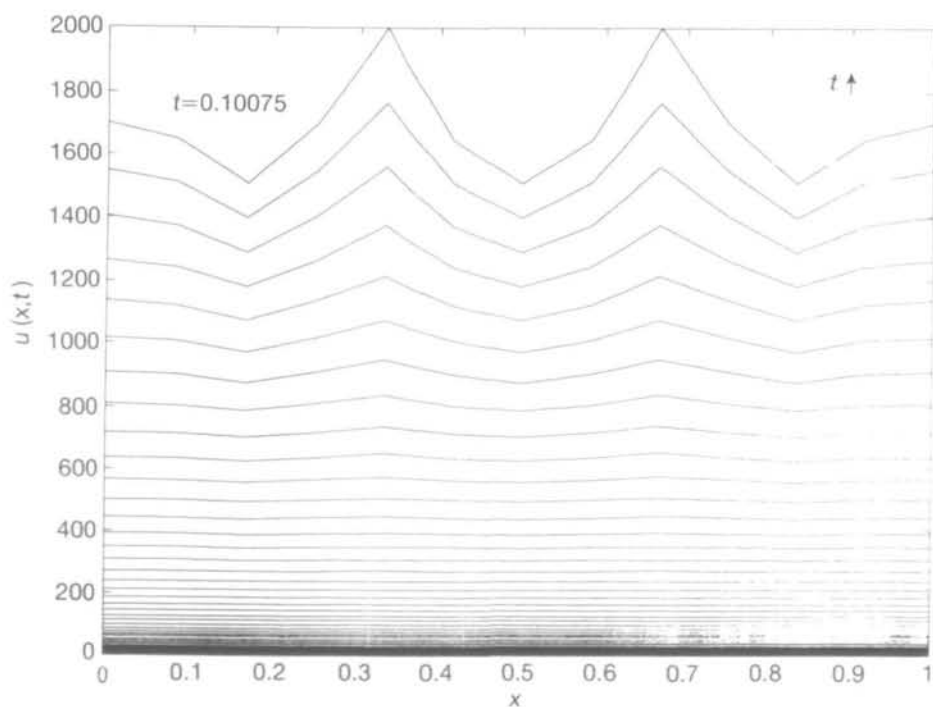


FIG. 8. Solutions of (PD), with  $J = 12$  and  $f(u) = 5u^3$ . Profiles at intervals of  $25\Delta t$

took a combination of the initial conditions for Figs 3 and 7, namely

$$U_j(0) = 1 + \frac{1}{2}10^{-5}(\cos(2\pi j/3) + \cos(\pi j/2)).$$

These data evolve into a spatial structure with period  $12\Delta x$ ; that is, the whole unit interval in  $x$ . This is the period which is the lowest common multiple of the periods of the two modes in the initial data. The results suggest that closed-form solutions are possible which represent the interaction of spurious  $3\Delta x$ - and  $4\Delta x$ -periodic modes with themselves and with the fundamental uniform mode.

The results shown in Figs 7 and 8 indicate that the three-mode solutions presented in section 3 do not represent the full range of nonlinear instabilities in (PD). A generalization of the analysis in section 2 shows that other closed forms, which could account for the phenomena in Figs 7 and 8, are indeed admitted by (PD). However, the resulting dynamical systems are of higher order than (2.6), (2.7) and more difficult to analyse. The simple equations we have studied in section 3 provide insight into the nature of the instabilities introduced by spatial discretization, aliasing, and nonlinear interaction without requiring complicated analysis.

Finally we discuss briefly the stability of the three-mode solution (2.1) as a solution of (PD). It is often the case that simple solutions such as (2.1) are themselves unstable to perturbations amongst other spatial modes (see [2, 3, 18] for discussion of this phenomenon in relation to discretizations of the inviscid

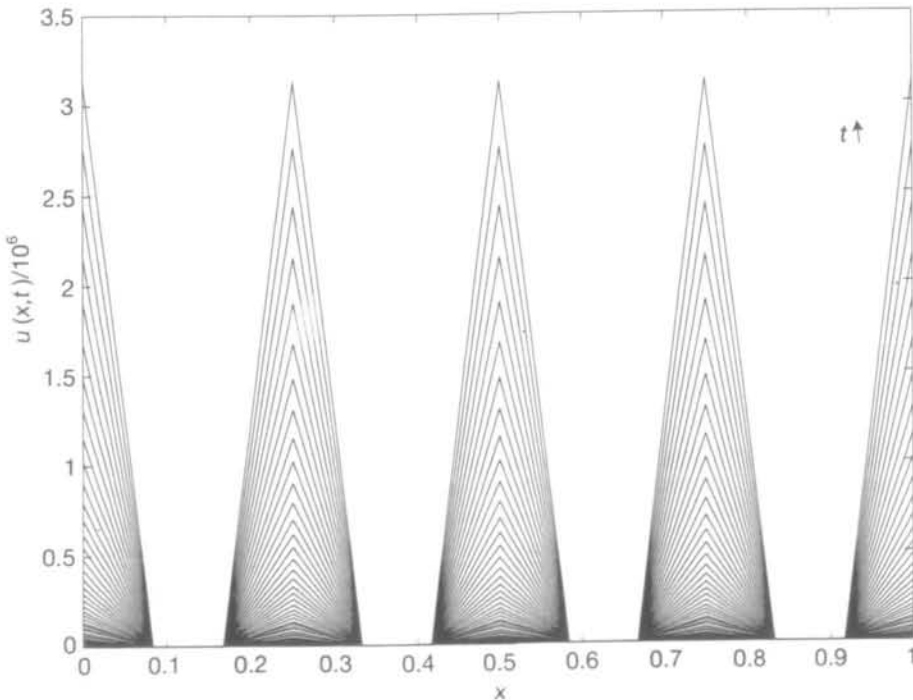


FIG. 9. As for Fig. 3 with twice as many time steps

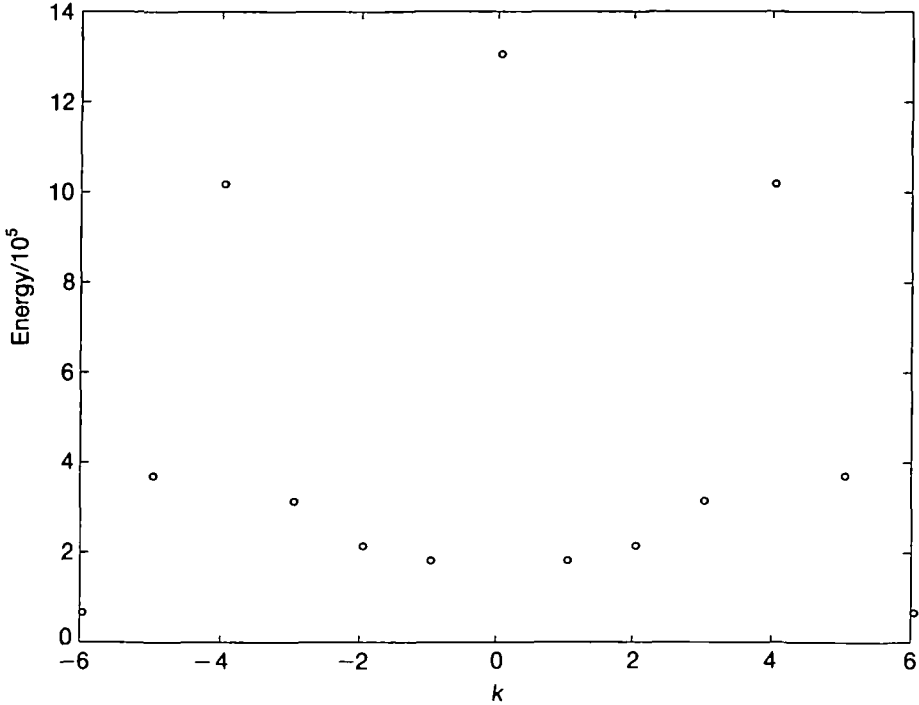


FIG. 10. Spectrum of the solution of (PD).  $J = 12$

Burgers' equation). This is the case here if solutions are integrated over a sufficiently large number of time steps. If (PD) is solved with identical data as for Fig. 3, but integrated for twice the number of time steps, then the solution develops pronounced spikes; see Fig. 9. Such spikes are characteristic of a solution in which all spatial modes are excited. This is confirmed in Fig. 10 which shows how much energy is in each mode  $\exp(2\pi ik/J)$ . Notice that the modes  $k=0$  and  $k=\pm 4$  are dominant, as we would expect from (2.1), but that energy has also leaked into all the remaining modes.

## 6. Conclusions

We have described an instability mechanism which arises in *spatial* discretizations of semilinear parabolic partial differential equations. The instability is manifest in problems which exhibit finite-time singularities, and it acts by destroying the spatial structure of the true solution close to the blow-up time. As the discussion of Figs 7 to 10 (in section 5) shows, the analysis of the simple solutions (2.1) does not cover all possible instabilities in (PD)—other modes can be stimulated by the initial data or by leakage of energy from the solution (2.1) to other spatial modes. However, the initial stages of the instability can be characterized generically by a *direct* transfer of energy from the physically meaningful low-wave-number modes to the spurious high-wave-number modes.

Our analysis is restricted to partial differential equations which admit spatially uniform solutions. However, it is likely that similar behaviour occurs in more general problems which admit singular solutions. The analysis of such problems is much more complicated and we believe that the concrete example constructed is valuable as a warning of some of the difficulties arising in the computation of singular solutions.

The work is also of independent interest since the conclusions are similar to those in [19], namely that high/low-wave-number interactions are crucial to the evolution of nonlinear instabilities in discrete parabolic equations. The assumptions and restrictions in [19] are quite different from those made here and so the two studies are complementary.

### Acknowledgements

I am grateful to both referees for suggestions which improved the presentation of this material.

### REFERENCES

1. BERGER, M., & KOHN, R. V. 1988 A rescaling algorithm for the numerical calculation of blowing up solutions. *Comm. pure appl. Math.* **41**, 841–863.
2. BRIGGS, W. L., NEWELL, A. C., & SARIE, T. 1983 Focusing: a mechanism for instability of nonlinear finite-difference equations. *J. Comp. Phys.* **51**, 83–106.
3. CLOOT, A., & HERBST, B. M. 1988 Grid resonances, focusing and Benjamin–Feir instabilities in leapfrog time discretisations. *J. Comp. Phys.* **75**, 31–53.
4. DOLD, J. W. 1985 Analysis of the early stages of thermal runaway. *Q. Jl. Mech. appl. Math.* **38**, 361–387.
5. DRAZIN, P. G., & REID, W. H. 1981 *Hydrodynamic Stability Theory*. Cambridge: University Press.
6. EASTWOOD, J. W., & ARTER, W. 1987 Spurious behaviour of numerically calculated fluid flow. *IMA J. numer. Anal.* **7**, 205–222.
7. FORNBERG, B. 1973 On the instability of Leap-Frog and Crank–Nicolson approximations of a nonlinear partial differential equation. *Math. Comp.* **27**, 45–57.
8. GIGA, Y., & KOHN, R. V. 1985 Asymptotically self-similar blowup of semilinear heat equations. *Comm. pure appl. Math.* **38**, 297–319.
9. HOCKING, L. M., STEWARTSON, K., & STUART, J. T. 1972 A nonlinear instability burst in plane parallel flow. *J. Fluid. Mech.* **51**, 705–735.
10. KAPILA, A. K. 1982 *Asymptotic Treatment Of Chemically Reacting Systems*. London: Pitman.
11. LACEY, A. A. 1981 The spatial dependence of supercritical reacting systems. *IMA J. appl. Math.* **27**, 71–84.
12. MATKOWSKY, B. J. 1970 A simple nonlinear dynamic stability problem. *Bull. Amer. math. Soc.* **76**, 620–625.
13. MITCHELL, A. R., & GRIFFITHS, D. F. 1986 Beyond the linear stability limit in nonlinear problems. *Numerical Analysis* (eds D. F. Griffiths & G. A. Watson). London: Pitman.
14. MOORE, D. W. 1983 Resonances introduced by discretization. *IMA J. appl. Math.* **31**, 1–11.
15. NEWELL, A. C. 1977 Finite amplitude instabilities of partial difference equations. *SIAM J. appl. Math.* **33**, 133–160.

16. PHILLIPS, N. A. 1959 An example of nonlinear computational instability. In: *The Atmosphere and the Sea in Motion* (ed. B. Bolin). Rockefeller Institute Press.
17. RICHTMYER, R. D. & MORTON, K. W. 1967 *Difference Methods For Initial Value Problems*. New York: Wiley.
18. SLOAN, D. M., & MITCHELL, A. R. 1986 On nonlinear instabilities in Leap-Frog finite difference schemes. *J. Comp. Phys.* **67**, 372–395.
19. STUART, A. M. 1988 Nonlinear instability in dissipative finite difference schemes. *SIAM Rev.*, to appear.
20. VADILLO, F., & SANZ-SERNA, J. M. 1986 Studies in numerical nonlinear instability. II. *J. Comp. Phys.* **66**, 225–238.